Applied Catalysis B: Environmental 325 (2023) 122371

Contents lists available at ScienceDirect

Applied Catalysis B: Environmental

journal homepage: www.elsevier.com/locate/apcatb

# New insights into peroxydisulfate activation by nanostructured and bulky carbons

Chenfei Shi *, Liyao Nie, Kai Hu, Chu Zheng, Chenmin Xu, Haiou Song, Guoxiang Wang

*School of Environment, Nanjing Normal University, Nanjing 210023, China*

ARTICLE INFO

*Keywords:*
Peroxydisulfate
Activated carbon
Carbon nanotube
Graphene nanoplatelet
4-Chlorophenol

ABSTRACT

Carbon-driven persulfate activation processes have attracted considerable attention because of their metal-free feature. However, the underlying mechanisms are not fully understood. In the study, biochar (WBC), activated carbon (PAC), carbon nanotube (CNT) and graphene nanoplatelet (GNP) were used as the activators of peroxydisulfate (PDS). Efficient removal of 4-chlorophenol (4-CP) was observed in the PAC/PDS, CNT/PDS and GNP/PDS systems. PAC performed better than CNT and GNP in both adsorption and activation. These three systems had identical reaction products and similar responses to the variation of reaction conditions, e.g., pH, concentrations of chloride and humic acid, indicated that the same mechanisms existed in them. The transformation of 4-CP went through two reaction pathways: direct oxidation by non-radical reactive species and carbon-mediated electron transfer. 4-CP molecules could be degraded or combined with each other to form dimers and trimers. These results provide a novel understanding of carbon-driven persulfate systems.

## 1. Introduction

Advanced oxidation processes (AOPs), involving the generation of high reactive oxygen species, have been considered as effective methods for the removal of refractory organic compounds in water. Persulfates (PS), including peroxymonosulfate (PMS) and peroxydisulfate (PDS), could be activated via the cleavage of O-O bonds to produce sulfate radicals ($SO_4\bullet^-$), which possess high redox potential (2.5−3.1 V) and long half-time period (30–40 μs) [1,2]. Furthermore, the oxidation processes based on $SO_4\bullet^-$ could be used in a wide range of pH (2−9) [3]. Thus, activated persulfate-based oxidation processes have received widespread attention in recent years. Approaches those have been used for persulfate activation include ultraviolet light irradiation [4], heat [5], ultrasound [6], alkaline [7], transition metal ions [8,9] and metal-containing composites [10–12]. Recently, increasing attention has been paid to persulfate oxidation processes driven by carbon materials (carbon/PS systems) because they are free from energy supply and metal ion leaching.

Sun et al. first reported that reduced graphene oxide could effectively activate PMS [13]. Afterwards, different nanostructured carbons, including nanodiamond, carbon nanotube and graphene, have been employed for persulfate activation. The activity of nanostructured carbon for PS activation is considered to originate from the carbon-conjugated structure, defective sites and proper amounts of functional groups [14]. In early studies, the removal of organic compounds in carbon/PS systems was ascribed to the role of free radicals [15,16]. Recent studies showed that the organic compounds could also be effectively degraded in some carbon/PS systems where no free radical was detected, so-called non-radical pathways [17,18]. Subsequently, numerous studies have focused on the optimal design of carbon materials and the identification of reaction pathways. The transformation mechanisms of organic compounds in carbon/PS systems are still not completely understood.

Activated carbon and biochar are typical bulky carbon materials, which have been used as adsorbent and soil improver respectively for decades. Recent studies showed that they could also been employed as the activators of persulfate [19,20]. Bulky carbons are more suitable for practical use than nanostructured carbons due to their low costs and ease of production. Both radical and non-radical pathways have been reported in the bulky carbon/PS systems, but the nature of PS activation by bulky carbons still remains unclear because of their complex composition and intricate structure.

In the study, several bulky (biochar and activated carbon) and nanostructured (carbon nanotube and graphene nanoplatelet) carbon materials were characterized and employed in carbon/PDS systems for the removal of 4-chlorophenol (4-CP), a refractory organic compound.

* Corresponding author.
*E-mail address:* schenfei@njnu.edu.cn (C. Shi).

https://doi.org/10.1016/j.apcatb.2023.122371
Received 1 September 2022; Received in revised form 18 December 2022; Accepted 3 January 2023
Available online 4 January 2023

The activities of carbon materials under different reaction conditions were investigated. The interactions between PDS and carbon materials were studied through quenching experiments, electron paramagnetic resonance (EPR) measurements, electrochemical analysis and theory calculations. The possible transformation pathways of 4-CP were proposed based on the identification of reaction products.

## 2. Materials and methods

### 2.1. Materials and chemicals

Wheat straw biochar and granular activated carbon were obtained from Sanli New Energy Co., Ltd. (Henan, China) and Norit Co., Ltd. (The Netherlands), respectively. Both of them were first crushed and passed through a 200-mesh sieve. Then powdered biochar (WBC) and activated carbon (PAC) were used in the carbon/PDS systems. Multi-walled carbon nanotube (CNT, >98% carbon basis), graphene nanoplatelet (GNP) and humic acid sodium salt (HA) were purchased from Sigma-Aldrich. 4-CP was obtained from Tokyo Chemical Industry (Japan). Sodium peroxydisulfate (PDS), sodium hydroxide (NaOH) and sodium chloride were supplied by Nanjing Chemical Reagent Co., Ltd. (Nanjing, China). Sulfuric acid ($H_2SO_4$), dimethyl sulfoxide (DMSO), furfuryl alcohol (FFA), sodium fluoride, 4-nitrophenol (4-NP) and phenol (PE) were purchased from Sinopharm Chemical Reagent Co., Ltd. (Shanghai, China). 5,5-Dimethyl-1-pyrroline N-oxide (DMPO) and 2,2,6,6-Tetramethyl-4-piperidone hydrochloride (TEMP) were obtained from Dojindo Laboratories (Japan).

### 2.2. Characterization

The morphologies and microstructure of carbon materials were observed by scanning electron microscopy (SEM; Apreo, Thermo Fisher Scientific, USA) and high-resolution transmission electron microscopy (HRTEM; Talos F200x, Thermo Fisher Scientific, USA). The surface areas and pore volumes of carbon materials were analyzed using Brunauer-Emmett-Teller (BET) method based on nitrogen adsorption-desorption isotherms at 77 K obtained from an Autosorb instrument (Quantachrome, USA). Pore size distribution was calculated using the DFT and BJH models. The crystal structures of carbon materials were detected by an X-ray diffractometer (Rigaku D/max 2500/PC, Japan). Defects of CNT and GNP were studied using confocal Raman spectroscopy (LabRAM HR Evolution, Horiba, France). The surface composition and element chemical states were characterized by X-ray photoelectron spectroscopy (XPS; ESCALAB $Xi^+$, Thermo Fisher Scientific, USA). The points of zero charge (pHzpc) were determined by the pH drift method [21].

### 2.3. Experimental procedure

Each experiment was conducted in a 250 mL conical flask containing 0.1 mmol/L of 4-CP solution. A certain amount of PDS was first dissolved in the solution, then the carbon material (WBC, PAC, CNT or GNP) was added into the flask and the mixture was mechanically stirred at 120 rpm at 25 °C. Initial pH of the solution was adjusted using $H_2SO_4$ or NaOH solution. At each time interval, 1 mL of solution was withdrawn and filtered through 0.22 μm micropore film for analysis. For the study of reaction products, the suspension containing carbon material was centrifuged at 2000 rpm for 30 min. Subsequently, the separated carbon material was extracted with methanol assisted by ultrasound in an ice-water bath. Then the obtained supernatant was collected for analysis.

### 2.4. Analytical methods

The concentration of 4-CP was determined using high-performance liquid chromatography (HPLC; Agilent 1290, USA) with a mobile phase consisting of methanol and 0.1% formic acid aqueous solution. The detection wavelengths for 4-CP, 4-NP and PE were 280 nm, 277 nm and 275 nm, respectively. The reaction products of 4-CP were identified by an ultra-high-performance liquid chromatographic system (UHPLC; UltiMate 3000, Thermo Fisher Scientific, USA) coupled with a LTQ-Orbitrap XL mass spectrometer (MS; Thermo Fisher Scientific, USA). The detailed conditions were listed in Text S1.

The concentration of sulfate ion in solution was measured by ion chromatography (ICS900, Dionex, USA). TOC analysis was performed using a multi N/C analyzer (HT 1300, Analytik Jena, Germany). The concentration of PDS was determined by the spectrophotometric method using a UV/Vis instrument (UV752N, Yoke instrument, China) [22]. EPR spectra were recorded using a Bruker E500 spectrometer. DMPO and TEMP were used as spin-trapping agents for free radicals ($SO_4\bullet^-$ and •OH) and $^1O_2$, respectively. Linear Sweep Voltammetry (LSV) measurements were conducted using a CHI 760E electrochemical analyzer (CH Instruments, Shanghai, China). Density functional theory (DFT) calculations and an independent gradient model (IGM) were used to study the adsorption behavior of PDS onto carbon materials. More detailed information for LSV measurements and DFT calculations can be found in Text S2 and Text S3, respectively.

## 3. Results and discussion

### 3.1. Characterization of carbon materials

The SEM images clearly showed the surface morphologies of carbon materials (Fig. 1). WBC exhibited a rough surface with several micro-sized pits, while the surface of PAC showed the accumulation of numerous particles with similar size. A network of wires could be observed in the image of CNT, while the morphology of GNP was more like a stack of sheets. HRTEM results demonstrated the internal structures of carbon materials (Fig. S1). The image of PAC was more inhomogeneous than WBC, indicated that it might have a loose and porous structure. Both the tubular structure of CNT and the layered structure of GNP could also be clearly observed in the images.

The surface areas of pore structures of carbon materials were then analyzed. As shown in Table 1 and Fig. S2, PAC had a surface area of 1449.2 $m^2/g$, which was significantly higher than those of other carbon materials. Furthermore, PAC exhibited a well-developed microporous structure, suggesting that it may have a good performance for 4-CP adsorption. WBC had the smallest surface area (61.3 $m^2/g$) and pore volume (0.1 $cm^3/g$) among the carbon materials. The pore volume of CNT was up to 2.3 $cm^3/g$, but it was mainly contributed by mesopores and macropores.

X-ray diffraction (XRD) patterns of carbon materials were illustrated in Fig. 2(a, b). The peaks on the pattern of WBC could be ascribed to several inorganic minerals, including quartz ($SiO_2$), sylvite (KCl) and calcite ($CaCO_3$). The pattern of GNP exhibited three peaks at $2\theta = 26.5°$, 42.9° and 54.8°, corresponding to (002), (100) and (004) crystal planes of graphite, respectively [23]. Two peaks at $2\theta = 26.5°$ and 42.9° could be observed on the pattern of CNT, while only a broad peak at around $2\theta = 26.7°$ appeared on the pattern of PAC. The intensity and number of peaks suggested the difference in the crystallinity of graphite in the carbon materials. The structural disorder of CNT and GNP were then characterized by confocal Raman spectroscopy. As shown in Fig. 2(c), two major peaks appearing at around 1577 $cm^{-1}$ (G band) and 1345 $cm^{-1}$ (D band) could be attributed to the stretching vibration mode of graphite crystals and disordered-induced mode, respectively. The $I_D/I_G$ values for CNT and GNP were respectively calculated as 1.24 and 0.72, indicating less graphitization or a higher defect level of CNT.

XPS wide-scan spectra of carbon materials were shown in Fig. 3(a). Two peaks locating at around 285 and 532 eV were observed, corresponding to C1s and O1s, respectively. Thus, carbon and oxygen were the main elements on the surface of the carbon materials. The O/C atomic ratios were 0.12, 0.12, 0.01 and 0.04 for WBC, PAC, CNT and GNP, respectively, indicating that bulky carbons contained less carbon and more oxygen than nanocarbons. The C1s spectra were deconvolved

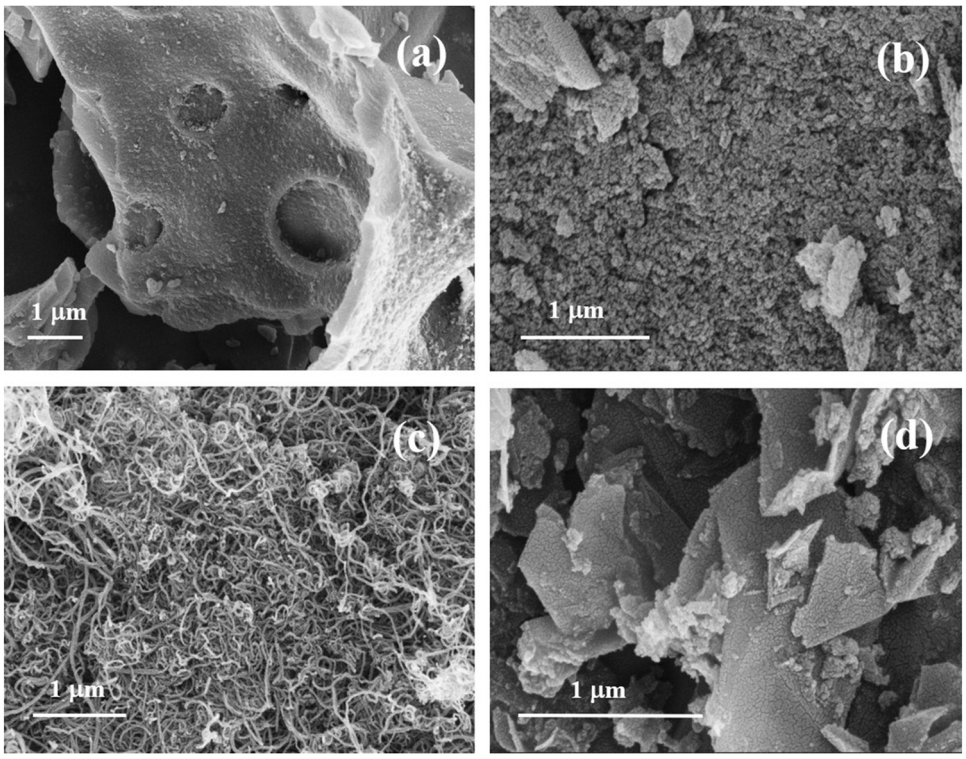


**Fig. 1.** SEM images of WBC (a), PAC (b), CNT (c) and GNP (d).

**Table 1**
Surface areas and pore volumes of carbon materials.

| Samples | BET surface area ($m^2/g$) | Micropore surface area ($m^2/g$) | Total pore volume ($P/P_0$ =0.99) ($cm^3/g$) | Average pore diameter (nm) |
|---|---|---|---|---|
| WBC | 61.3 | 11.8 | 0.1 | 6.2 |
| PAC | 1449.2 | 729.8 | 1.4 | 3.7 |
| CNT | 225.1 | — | 2.3 | 40.1 |
| GNP | 329.4 | 47.1 | 0.7 | 8.8 |

into five peaks at 284.7 ± 0.1, 285.3 ± 0.1, 286.5 ± 0.1, 288.9 and 291.2 eV, corresponding to C graphite/C−C/C−H, C−OH/C−O−C, C═O, COOH and π − π * shake up, respectively [24,25]. As depicted in Fig. 3(b–e), different distribution could be observed in the C1s spectra. Less C graphite/C−C/C−H and more C−OH/C−O−C existed on the surface of bulky carbons.

### 3.2. Removal of 4-CP in carbon/PDS systems

In the study, PDS alone (1 mmol/L) exhibited ignorable reactivity towards 4-CP (0.1 mmol/L) and only less than 4% of 4-CP could be degraded. The WBC/PDS system also performed poorly, with the efficiency of 8.8% at 240 min (Fig. 4(a)). Such efficiency could be easily achieved by adsorption, suggesting that WBC was not suitable for PDS activation.

Efficient removal of 4-CP was observed in PAC/PDS, CNT/PDS and GNP/PDS systems (Fig. 4(b–d)). 4-CP could be partly removed by adsorption onto PAC, CNT and GNP, the process nearly reached equilibrium within 60 min. The adsorption capacity of CNT was significantly lower than those of PAC and GNP. After the addition of PDS at 60 min, it was activated by carbon materials and 4-CP was further removed. Adsorption allowed enrichment of 4-CP on carbon surface and increased its subsequent removal rate. However, the addition time of PDS had no significant effect on the removal efficiency of 4-CP at 240 min, which may be due to the limited number of active sites. The pseudo-first-order rate constants ($k_{obs}$) were 0.017 $min^{-1}$ ($R^2$ = 0.976), 0.0058 $min^{-1}$ ($R^2$ = 0.987) and 0.0146 $min^{-1}$ ($R^2$ = 0.987) for PAC/PDS, CNT/PDS and GNP/PDS, respectively. It is worth noting that the addition of PDS decreased the pH of the solution to 3.0, which may affect the adsorption of 4-CP. Therefore, the removal processes of 4-CP by adsorption onto carbon materials at pH 3.0 (adjustment with $H_2SO_4$ solution) were investigated. As shown in Fig. 4(b–d), the change in pH had almost no effect on the adsorption efficiency of 4-CP, confirming that the main role of PDS in these systems was involved in the transformation of 4-CP.

### 3.3. Effect of pH on the 4-CP removal in carbon/PDS systems

The pH of the solution is usually considered to be an important factor affecting adsorption and advanced oxidation processes. In the study, pH exerted a similar influence on the removal of 4-CP in different carbon/PDS systems (Fig. 5). That is, the kinetic process did not change much under acidic (pH 3.0) and neutral conditions (pH 7.0), while it was significantly inhibited under alkaline condition (pH 11.0). This might be due to the electrostatic interaction between carbon materials and 4-CP. The dissociation constant (pKa) of 4-CP was about 9.4, indicating that some 4-CP molecules would dissociate into anions at 11.0. The pHzpc values of PAC, CNT and GNP were 2.3, 7.2 and 4.2, respectively. Thus, all of the carbon materials were negatively charged at pH 11.0, which would exhibit electrostatic repulsion and inhibit the adsorption of 4-CP onto the carbon surface. This hypothesis was also confirmed by comparing the adsorption efficiency at pH 3.0 and pH 11.0 (Fig. S3). Alkaline condition had a smaller impact on CNT/PDS system, which may be related to the weaker electrostatic repulsion between CNT and 4-CP and the lower adsorption capacity of CNT.

### 3.4. Effects of HA and $Cl^-$ on the 4-CP removal in carbon/PS systems

Dissolved organic matter (DOM) and halogen anions, which are widely present in the environment, have been reported to be important factors influencing persulfate activation processes [26]. Therefore, the

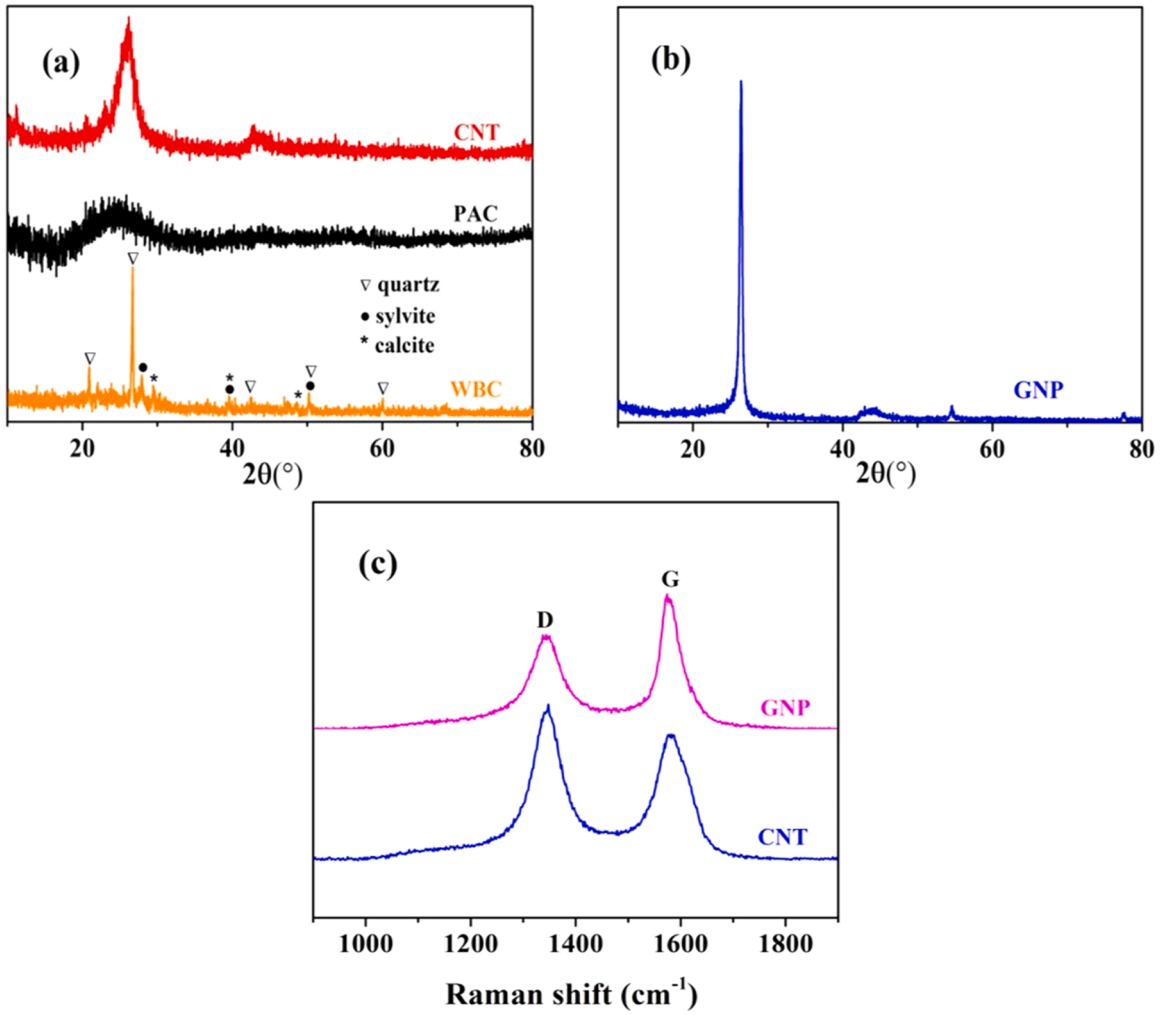


**Fig. 2.** XRD patterns (a, b) and Raman spectra (c) of carbon materials.

effects of HA (a major constituent of DOM) and $Cl^-$ on the 4-CP removal in carbon/PDS systems were investigated in the study. As shown in Fig. 6 (a), the removal efficiency of 4-CP decreased when HA was added into the systems and higher concentration of HA exerted a greater negative effect. This may be due to the HA adsorption onto the carbon surface, resulting in blocking the pores or covering the sites for 4-CP adsorption. Furthermore, HA could also act as a competitor in the systems through consuming PS or radicals [27]. In addition to DOM, previous studies have reported that $Cl^-$ could react with the free radicals to form a series of halogen radicals, which will reduce the degradation efficiency of organic compounds in the persulfate-based oxidation processes [28]. However, in the study, the decline in the 4-CP removal upon the addition of $Cl^-$ (0.5 and 5 mmol/L) was insignificant (Fig. 6(b)), indicating that free radicals may not play a decisive role in carbon/PDS systems.

### 3.5. Identification of oxidizing species

A high dosage of methanol (methanol/PDS molar ratio 988.5/1) was added into carbon/PDS systems to confirm whether the free radicals were involved in the degradation of 4-CP. As shown in Fig. 7(a), methanol had a negligible effect on the 4-CP removal in carbon/PDS systems. Moreover, the EPR analysis with DMPO in Fig. 8(a) did not show the signals of DMPO-OH and DMPO-$SO_4$, confirming the absence of free radicals in the solution. Then DMSO was added into the systems to explore the possibility of the presence of surface-bound radicals [29]. As shown in Fig. 7(b), the removal of 4-CP was also hardly affected by the addition of DMSO. Furthermore, several studies have shown that $F^-$ could desorb surface-bound free radicals into solution [30,31]. However, the addition of NaF in the study did not lead to the appearance of free radical signals (Fig. 8(a)). Therefore, surface-bound free radicals did not play an important role in the 4-CP removal.

Notably, the characteristic peaks of DMPO oxidation product (DMPO-X) appeared in the EPR spectra (Fig. 8(a)), suggesting the generation of oxidizing species through the reactions between PDS and carbon materials. Similar signal was observed in the study of Lee et al., which was attributed to the formation of reactive complexes with PDS bound onto the surface of carbon material [17]. These complexes could oxidize organic compounds via electron abstraction. The results in Fig. 9 confirmed the consumption of PDS in the study, which also indicated the generation of $SO_4^{2-}$ during the reaction between PDS and carbon materials. Therefore, PDS was not simply compounded with carbon materials but reacted with them to form oxidizing species, accompanied by the release of $SO_4^{2-}$. Furthermore, a positive correlation could be obtained between $SO_4^{2-}$ release (or the consumption of PDS) and the pseudo-first-order rate constants ($R^2 > 0.94$), suggesting that the reactions between PDS and carbon materials played an important role in the removal of 4-CP. The stability of the oxidizing species was then investigated by mixing the carbon materials and PDS in 10 mL water for 5 min before adding them into 4-CP solution. As shown in Fig. S4, premixing had little effect on the removal of 4-CP, indicating that the oxidizing species was more stable than free radicals and had a longer half-life period.

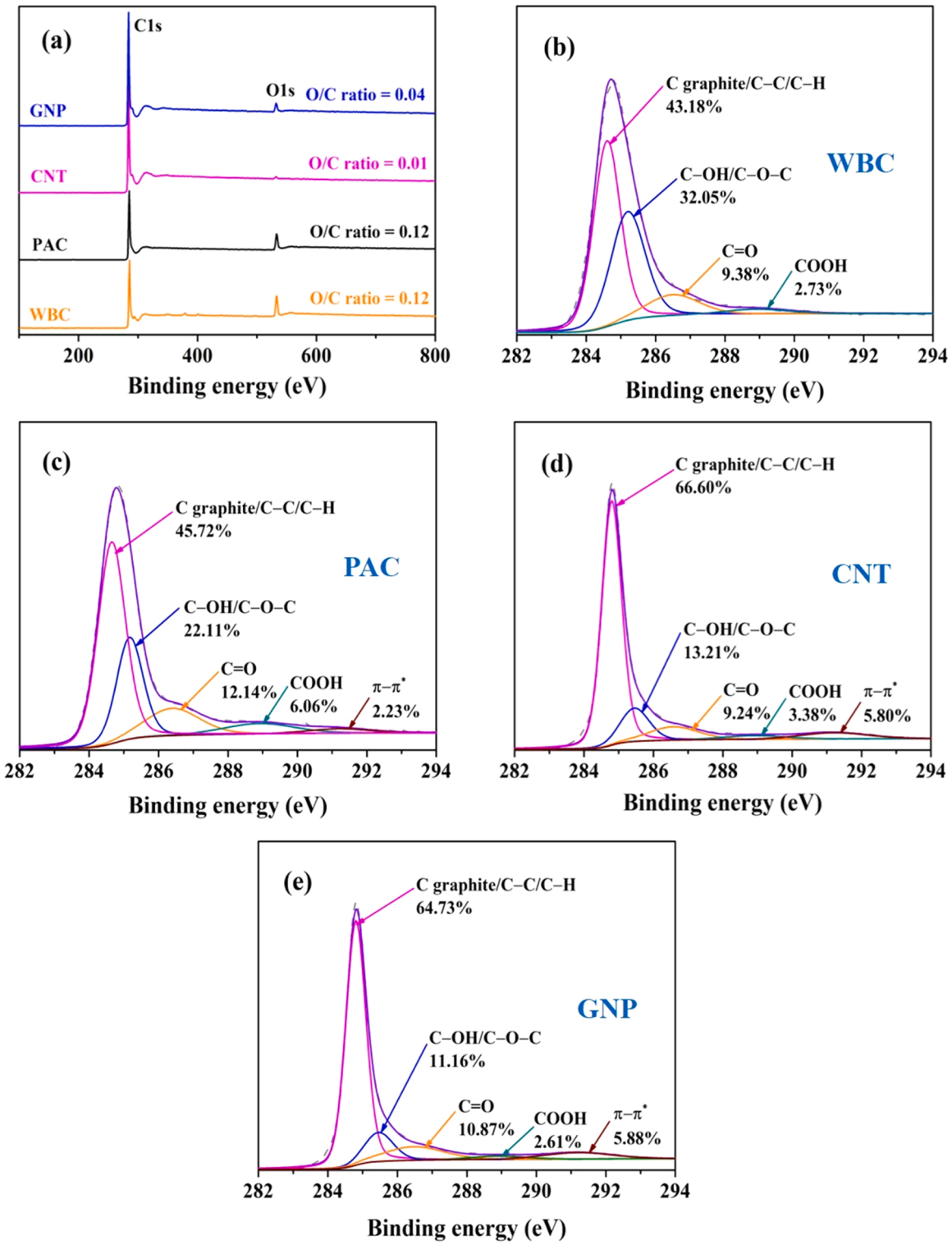


**Fig. 3.** XPS wide-scan (a) and C1s spectra (b−e) of carbon materials.

FFA was used as the scavenger to confirm the generation of $^1O_2$ in carbon/PDS systems. As illustrated in Fig. 7(c), the addition of FFA significantly suppressed the removal of 4-CP in all the systems. Since FFA had almost no effect on the adsorption of 4-CP (Fig. S3), it might influence the transformation of 4-CP in the systems. However, FFA could be effectively oxidized via reaction with PS and the electron-transfer process [32]. The inhibitory effect of FFA observed in the study could not be taken as convincing evidence for the generation of $^1O_2$. EPR analysis with TEMP was then carried out to verify the generation of $^1O_2$. No characteristic signal was observed in the EPR spectra of carbon/PDS systems (Fig. 8(b)), ruling out the role of $^1O_2$ in the degradation of 4-CP.

Another possible mechanism in the systems is direct electron transfer from organic compounds (donor) to persulfate (acceptor) with the carbon materials acting as the mediators. In case such a reaction mechanism, the addition of 4-CP will affect the consumption of PDS and the generation of $SO_4^{2-}$. As shown in Fig. 9, the addition of 4-CP in carbon/

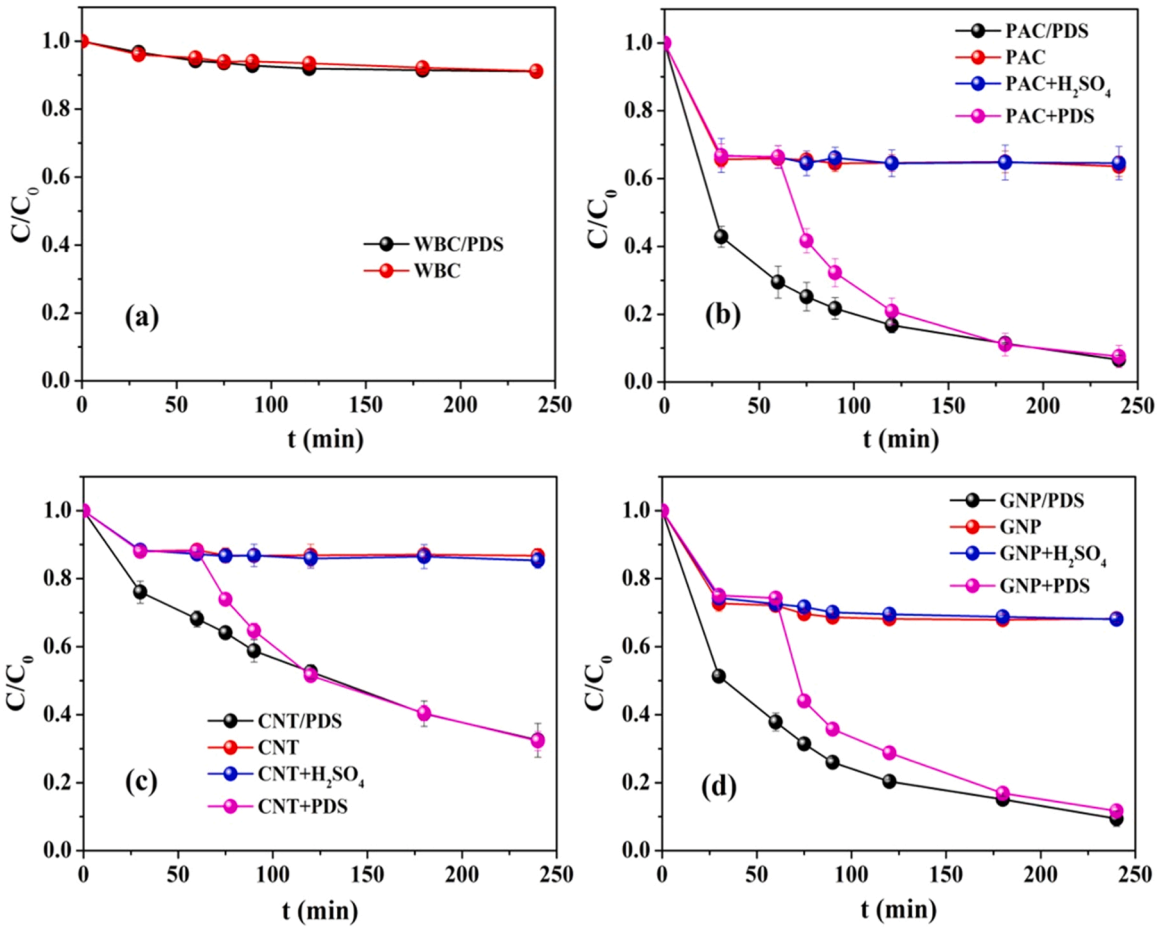


**Fig. 4.** 4-CP removal in carbon/PDS systems ("Carbon/PDS" represents that carbon and PDS were added together into 4-CP solution at 0 min "Carbon+PDS" or "Carbon+$H_2SO_4$" represents that carbon was added into the solution at 0 min and then PDS or $H_2SO_4$ was added at 60 min. Reaction conditions: 0.1 mmol/L 4-CP; 0.1 g/L carbon material; 1 mmol/L PDS).

PDS systems promoted the decomposition of PDS and the release of $SO_4^{2-}$ although PDS itself could decompose to produce a small amount of $SO_4^{2-}$. This indicated that electron transfer played a role in the degradation of 4-CP. Furthermore, according to the LSV curves in Fig. S5, the addition of 4-CP brought about an increase in the electrochemical current, which meant that the electron transfer from 4-CP to carbon-coated electrode occurred. These results confirmed the electron transfer reactions in the carbon/PDS systems. Notably, electron transfer mechanism assumes that persulfate is consumed only by organic compounds. However, in the study, the decomposition of PDS and the release of $SO_4^{2-}$ remained significant in the absence of 4-CP. Moreover, the increase in $SO_4^{2-}$ caused by the addition of 4-CP was confusing and such weak facilitation in GNP/PDS system could hardly explain the rapid removal of 4-CP. Both of them suggested the existence of other reaction mechanisms. Combined with the results in Fig. 8(a), the transformation of 4-CP in carbon/PDS systems went through two pathways: oxidation by reactive species and carbon-mediated electron transfer from 4-CP to PDS.

Then two additional phenols, 4-NP and PE, were selected as the target organic compounds to investigate the suitability of the carbon/PDS systems. As shown in Fig. S6, the carbon materials exhibited different adsorption performances for the phenols (0–60 min). However, the removal of the phenols showed a same trend after PDS was added, with the rate following the order 4-CP > PE > 4-NP, which was consistent with the order of the electron-donating abilities of the phenols [32]. Thus, the carbon/PDS systems were more effective for the phenol with stronger electron-donating ability.

### 3.6. Role of carbon materials

In the study, the system with higher surface area carbon material exhibited better performance in the removal of 4-CP, which can be explained by the enrichment of 4-CP and PDS on the carbon surface, shortening the distances and increasing the reaction rates among them. Then Amberlite XAD4 (Rohm and Haas Company), an adsorption resin with high surface area (≧750 $m^2/g$) but without carbon matrix and functional groups, was employed to verify the role of interface. As illustrated in Fig. S7, the resin could effectively remove 4-CP by adsorption, but hardly activate PDS, suggesting that only the interface was not enough to trigger the transformation of 4-CP and additional active sites were required.

In carbon/PS systems, the degradation of organic compounds was usually attributed to carbon matrix (graphitized carbons, defects) and surface functional groups [33,34]. PAC had lower graphitized crystallinity than CNT and GNP, but sufficient functional groups may allow it exhibit great activation performance for PDS. Since XPS results showed that more C–OH/C–O–C existed on the surface of bulky carbons, density functional theory (DFT) calculations and IGM analysis were used to examine the adsorption behavior of PDS onto carbon matrix with these two functional groups (Fig. S8). Since previous studies have reported that the oxygen groups located on the edge of the graphene layer were more active than those at the base plane, the oxygen-containing groups (C–OH and C–O–C) were placed at the edge of graphene in the study [35]. The adsorption energies were respectively calculated as − 0.21 eV (edge), − 0.26 eV (edge with C-OH) and − 0.22 eV (edge with C-O-C), confirming that these two groups were beneficial to PDS

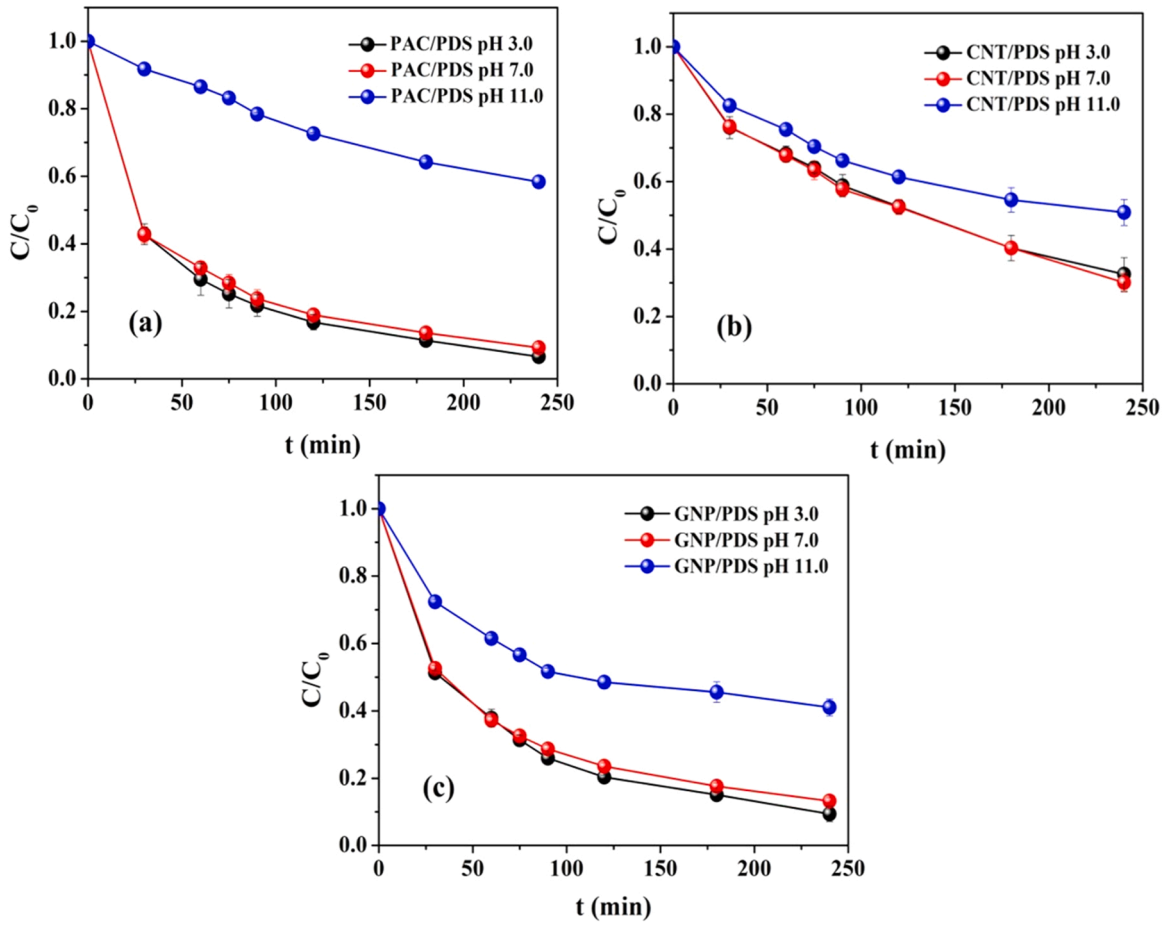


**Fig. 5.** Effect of pH on the removal of 4-CP in carbon/PDS systems (Reaction conditions: 0.1 mmol/L 4-CP; 0.1 g/L carbon material; 1 mmol/L PDS).

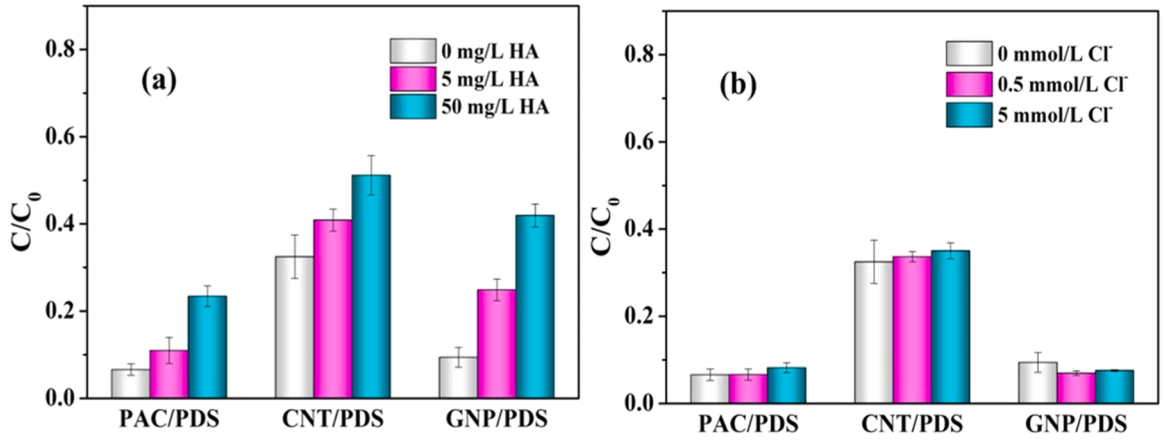


**Fig. 6.** Effects of HA (a) and $Cl^-$ (b) on the removal of 4-CP in carbon/PS systems (Reaction conditions: 0.1 mmol/L 4-CP; 0.1 g/L carbon material; 1 mmol/L PDS; no pH adjustment).

adsorption on carbon materials.

### 3.7. Reaction products analysis

TOC and $Cl^-$ of the solution at 240 min were monitored. The results showed that 44.3−55.8% of TOC was removed and 26.5−32.7% of chlorine on 4-CP molecules was converted into $Cl^-$. Previous studies have reported two main pathways for 4-CP degradation in the photocatalytic oxidation systems: substitution to form hydroquinone and hydroxylation to form 4-chlorocatechol [36]. In the study, 1,4-benzoquinone, 4-chlorocatechol, 2-hydroxy-1,4-benzoquinone and high-molecular-weight products ($m/z = 252.98$ and 378.97) were detected in the carbon/PDS systems (Fig. S9–S11). These high-molecular-weight products were supposed to be cross-coupling dimers and trimers. According to all above results, the possible pathways for 4-CP transformation were proposed (Fig. 10). For the first process, 4-CP is converted to hydroquinone by hydrolytic dechlorination or 4-chlorocatechol by hydroxylation, and then oxidized to 2-hydroxy-1,

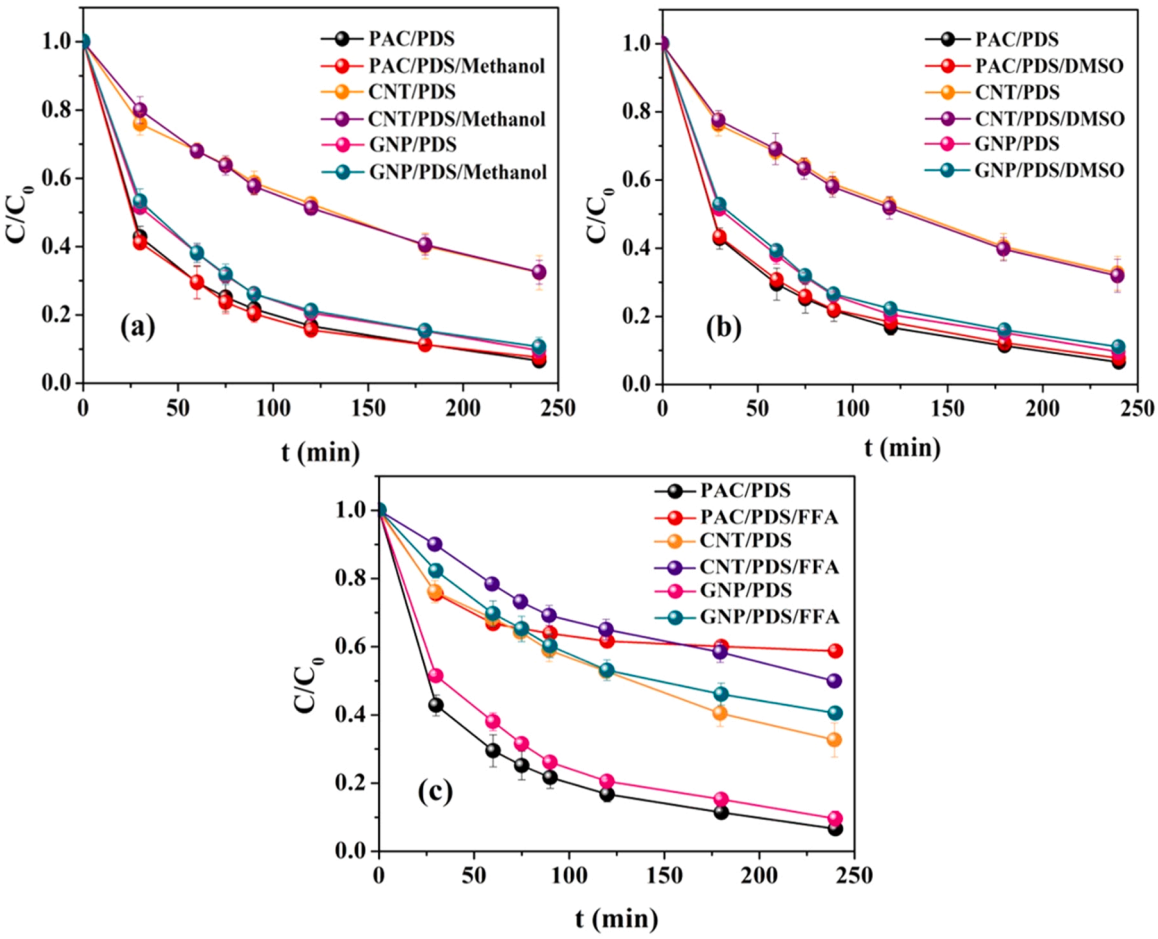


**Fig. 7.** Effects of methanol (a), DMSO (b) and FFA (c) on the removal of 4-CP in carbon/PDS systems (Reaction conditions: 0.1 mmol/L 4-CP; 0.1 g/L carbon material; 1 mmol/L PDS; 988.5 mmol/L methanol; 8 mmol/L DMSO; 1 mmol/L FFA; no pH adjustment).

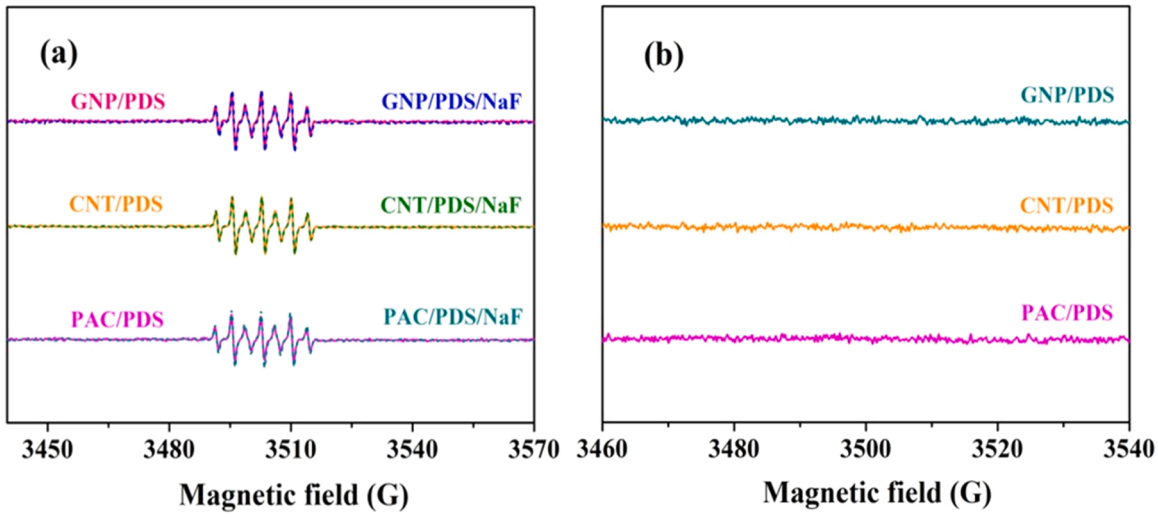


**Fig. 8.** EPR spectra for $SO_4^{\bullet-}$/•OH (a) and $^1O_2$ (b) of the carbon/PDS systems (Reaction conditions: 1 g/L carbon material; 10 mmol/L PDS; 100 mmol/L DMPO; 100 mmol/L TEMP; 2 mmol/L NaF; no pH adjustment; reaction time = 5 min).

4-benzoquinone. The benzene ring in 2-hydroxy-1,4-benzoquinone is easily opened to form organic acids, which can be further mineralized into $CO_2$ and $H_2O$. For the second process, electrons are transferred from 4-CP to the oxidizing species (or carbon material) and phenoxyl radicals can be generated by the delocalization of the unpaired electron. Subsequently, dimers and trimers are formed through C-O and C-C coupling between phenoxyl radicals. Notably, no dechlorination was observed during the coupling process. The generation of $Cl^-$ in carbon/PDS systems indicated that the first process played an important role in the removal of 4-CP.

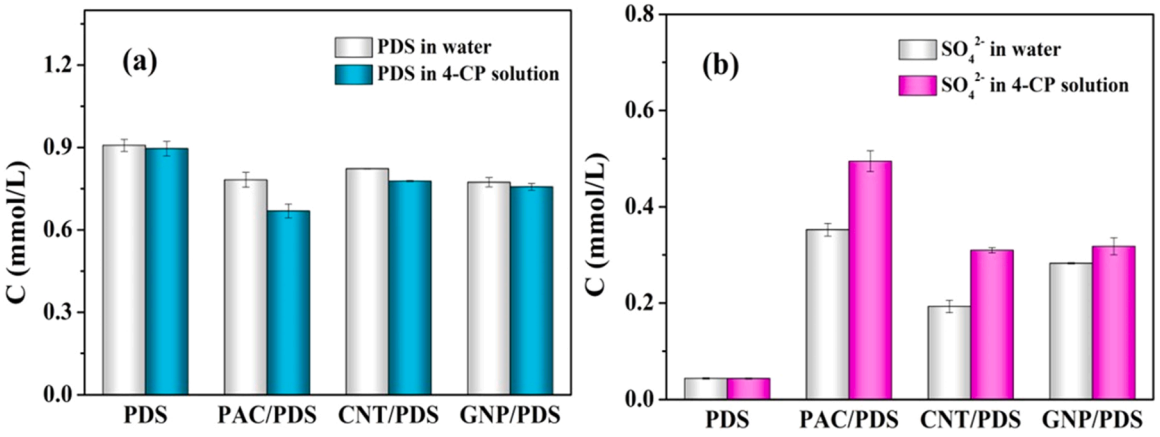


**Fig. 9.** Decomposition of PDS (a) and release of $SO_4^{2-}$ (b) in carbon/PDS systems (Reaction conditions: 0.1 mmol/L 4-CP; 0.1 g/L carbon material; 1 mmol/L PDS).

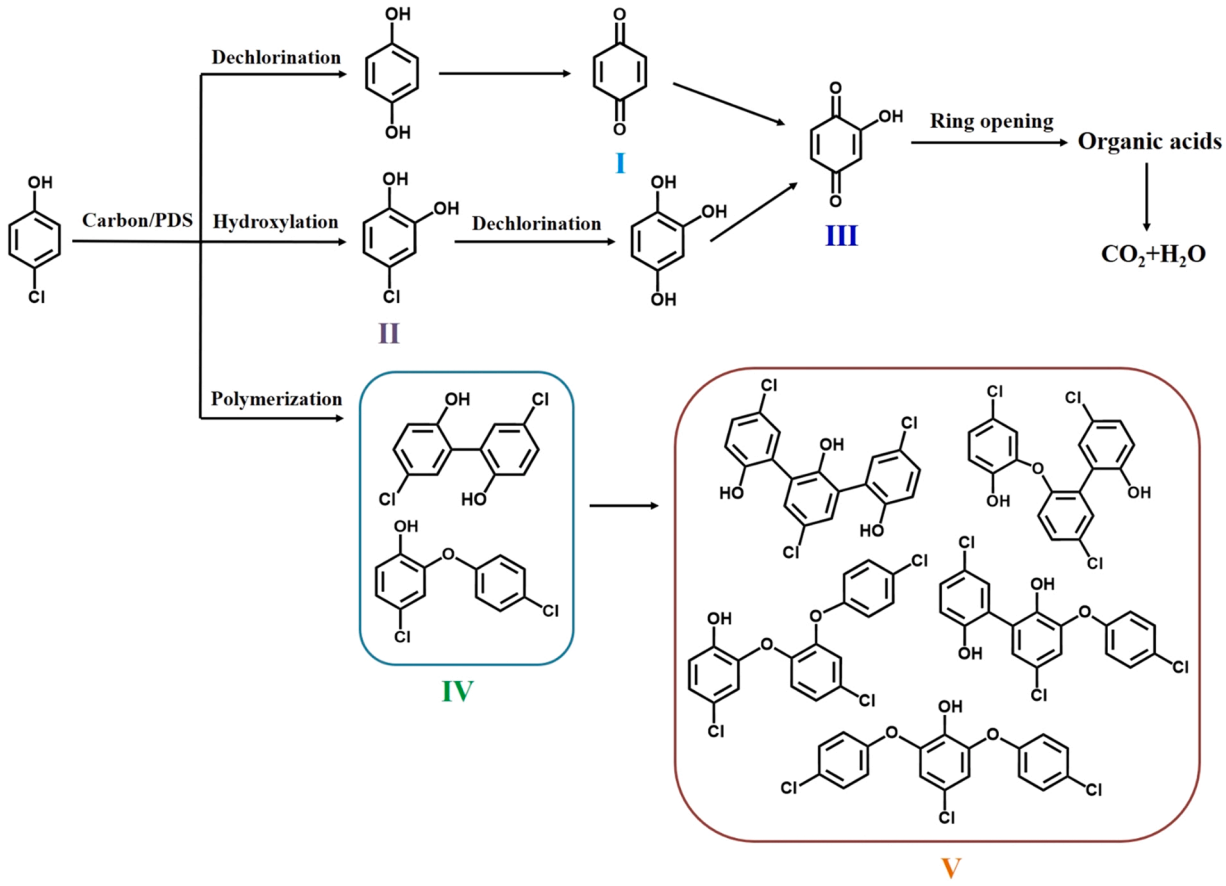


**Fig. 10.** Proposed pathways for 4-CP transformation in carbon/PDS systems.

## 4. Conclusions

In the study, removal performances and mechanisms of 4-CP in different carbon/PDS systems were investigated. The PAC/PDS, CNT/PDS and GNP/PDS systems can remove 4-CP rapidly, while WBC could hardly activate PDS. Alkaline condition and high concentration of humic acid inhibited the removal of 4-CP. Enrichment on the surface by adsorption was a necessary but not sufficient condition for the transformation of 4-CP. Additional active sites (surface functional groups and carbon matrix) were required. Free radicals ($SO_4^{\bullet-}$ and •OH) and singlet oxygen were not detected and novel oxidizing species could be generated through the reactions between PDS and carbon materials. Carbon mediated-electron transfer also played a role in the removal of 4-CP. In carbon/PDS systems, 4-CP could be degraded into small molecules or polymerized to form oligomers.

## CRediT authorship contribution statement

**Chenfei Shi**: Writing – original draft, Supervision. **Liyao Nie**: Investigation, Methodology. **Kai Hu**: Investigation. **Chu Zheng**: Investigation. **Chenmin Xu**: Writing – review & editing. **Haiou Song:** Writing – review & editing. **Guoxiang Wang**: Funding acquisition.

## Declaration of Competing Interest

The authors declare that they have no known competing financial interests or personal relationships that could have appeared to influence the work reported in this paper.

## Data availability

Data will be made available on request.

## Acknowledgments

This work was supported by the Jiangsu Agricultural Science and Technology Innovation Fund, China (Grant No. CX(21)3165).

## Appendix A. Supplementary material

Supplementary data associated with this article can be found in the online version at doi:10.1016/j.apcatb.2023.122371.

## References

[1] P. Hu, M. Long, Cobalt-catalyzed sulfate radical-based advanced oxidation: a review on heterogeneous catalysts and applications, Appl. Catal. B Environ. 181 (2016) 103–117.
[2] J. Wang, S. Wang, Activation of persulfate (PS) and peroxymonosulfate (PMS) and application for the degradation of emerging contaminants, Chem. Eng. J. 334 (2018) 1502–1517.
[3] W.-D. Oh, Z. Dong, T.-T. Lim, Generation of sulfate radical through heterogeneous catalysis for organic contaminants removal: current development, challenges and prospects, Appl. Catal. B Environ. 194 (2016) 169–201.
[4] L. Xian, Y. Shao, N. Gao, J. Chen, H. Deng, W. Chu, A. Na, F. Peng, Investigation of clofibric acid removal by UV/persulfate and UV/chlorine processes: kinetics and formation of disinfection byproducts during subsequent chlor(am)ination, Chem. Eng. J. 331 (2018) 364–371.
[5] Y. Fan, Y. Ji, D. Kong, J. Lu, Q. Zhou, Kinetic and mechanistic investigations of the degradation of sulfamethazine in heat-activated persulfate oxidation process, J. Hazard. Mater. 300 (2015) 39–47.
[6] Z. Wei, F.A. Villamena, L.K. Weavers, Kinetics and mechanism of ultrasonic activation of Persulfate: an in situ EPR spin trapping study, Environ. Sci. Technol. 51 (2017) 3410–3417.
[7] M.A. Lominchar, A. Santos, E. de Miguel, A. Romero, Remediation of aged diesel contaminated soil by alkaline activated persulfate, Sci. Total Environ. 622–623 (2018) 41–48.
[8] G.P. Anipsitakis, D.D. Dionysiou, Radical generation by the interaction of transition metals with common oxidants, Environ. Sci. Technol. 38 (2004) 3705–3712.
[9] Z. Yan, Y. Gu, X. Wang, Y. Hu, X. Li, Degradation of aniline by ferrous ions activated persulfate: impacts, mechanisms, and by-products, Chemosphere 268 (2021), 129237.
[10] J. Ali, L. Wenli, A. Shahzad, J. Ifthikar, G.G. Aregay, I.I. Shahib, Z. Elkhlifi, Z. Chen, Z. Chen, Regulating the redox centers of Fe through the enrichment of Mo moiety for persulfate activation: a new strategy to achieve maximum persulfate utilization efficiency, Water Res. 181 (2020), 115862.
[11] R. Guan, X. Yuan, Z. Wu, L. Jiang, J. Zhang, Y. Li, G. Zeng, D. Mo, Efficient degradation of tetracycline by heterogeneous cobalt oxide/cerium oxide composites mediated with persulfate, Sep. Purif. Technol. 212 (2019) 223–232.
[12] M. Ouyang, X. Li, Q. Xu, Z. Tao, F. Yao, X. Huang, Y. Wu, D. Wang, Q. Yang, Z. Chen, Z. Pi, Heterogeneous activation of persulfate by Ag doped $BiFeO_3$ composites for tetracycline degradation, J. Colloid Interface Sci. 566 (2020) 33–45.
[13] H. Sun, S. Liu, G. Zhou, H.M. Ang, M.O. Tadé, S. Wang, Reduced graphene oxide for catalytic oxidation of aqueous organic pollutants, ACS Appl. Mater. Interfaces 4 (2012) 5466–5471.
[14] X. Duan, H. Sun, J. Kang, Y. Wang, S. Indrawirawan, S. Wang, Insights into heterogeneous catalysis of persulfate activation on dimensional-structured nanocarbons, ACS Catal. 5 (2015) 4629–4636.
[15] S. Indrawirawan, H. Sun, X. Duan, S. Wang, Nanocarbons in different structural dimensions (0–3D) for phenol adsorption and metal-free catalytic oxidation, Appl. Catal. B Environ. 179 (2015) 352–362.
[16] H. Sun, C. Kwan, A. Suvorova, H.M. Ang, M.O. Tadé, S. Wang, Catalytic oxidation of organic pollutants on pristine and surface nitrogen-modified carbon nanotubes with sulfate radicals, Appl. Catal. B Environ. 154–155 (2014) 134–141.
[17] H. Lee, H.-J. Lee, J. Jeong, J. Lee, N.-B. Park, C. Lee, Activation of persulfates by carbon nanotubes: oxidation of organic compounds by nonradical mechanism, Chem. Eng. J. 266 (2015) 28–33.
[18] S. Zhu, C. Jin, X. Duan, S. Wang, S.-H. Ho, Nonradical oxidation in persulfate activation by graphene-like nanosheets (GNS): differentiating the contributions of singlet oxygen ($^1O_2$) and sorption-dependent electron transfer, Chem. Eng. J. 393 (2020), 124725.
[19] V.L. Pham, D.-G. Kim, S.-O. Ko, Advanced oxidative degradation of acetaminophen by carbon catalysts: radical vs non-radical pathways, Environ. Res. 188 (2020), 109767.
[20] Z. Feng, B. Zhou, R. Yuan, H. Li, P. He, F. Wang, Z. Chen, H. Chen, Biochar derived from different crop straws as persulfate activator for the degradation of sulfadiazine: influence of biomass types and systemic cause analysis, Chem. Eng. J. 440 (2022), 135669.
[21] R.S. Ribeiro, A.M.T. Silva, J.L. Figueiredo, J.L. Faria, H.T. Gomes, Removal of 2-nitrophenol by catalytic wet peroxide oxidation using carbon materials with different morphological and chemical properties, Appl. Catal. B Environ. 140–141 (2013) 356–362.
[22] C. Liang, C.-F. Huang, N. Mohanty, R.M. Kurakalva, A rapid spectrophotometric determination of persulfate anion in ISCO, Chemosphere 73 (2008) 1540–1543.
[23] E. Voss, B. Vigolo, G. Medjahdi, C. Hérold, J.-F. Marêché, J. Ghanbaja, F. Le Normand, V. Mamane, Covalent functionalization of polyhedral graphitic particles synthesized by arc discharge from graphite, Phys. Chem. Chem. Phys. 19 (2017) 5405–5410.
[24] L. Tang, Y. Liu, J. Wang, G. Zeng, Y. Deng, H. Dong, H. Feng, J. Wang, B. Peng, Enhanced activation process of persulfate by mesoporous carbon for degradation of aqueous organic pollutants: electron transfer mechanism, Appl. Catal. B Environ. 231 (2018) 1–10.
[25] A.P. Terzyk, The influence of activated carbon surface chemical composition on the adsorption of acetaminophen (paracetamol) in vitro Part II. TG, FTIR, and XPS analysis of carbons and the temperature dependence of adsorption kinetics at the neutral pH, Colloids Surf. A Physicochem. Eng. Asp. 177 (2001) 23–45.
[26] W. Huang, S. Xiao, H. Zhong, M. Yan, X. Yang, Activation of persulfates by carbonaceous materials: a review, Chem. Eng. J. 418 (2021), 129297.
[27] Y. Shi, J. Zhu, G. Yuan, G. Liu, Q. Wang, W. Sun, B. Zhao, L. Wang, H. Zhang, Activation of persulfate by EDTA-2K-derived nitrogen-doped porous carbons for organic contaminant removal: radical and non-radical pathways, Chem. Eng. J. 386 (2020), 124009.
[28] Y. Gao, Q. Wang, G. Ji, A. Li, Degradation of antibiotic pollutants by persulfate activated with various carbon materials, Chem. Eng. J. 429 (2022), 132387.
[29] D.T. Oyekunle, B. Wu, F. Luo, J. Ali, Z. Chen, Synergistic effects of Co and N doped on graphitic carbon as an in situ surface-bound radical generation for the rapid degradation of emerging contaminants, Chem. Eng. J. 421 (2021), 129818.
[30] G. Fang, Y. Deng, M. Huang, D.D. Dionysiou, C. Liu, D. Zhou, A mechanistic understanding of hydrogen peroxide decomposition by vanadium minerals for diethyl phthalate degradation, Environ. Sci. Technol. 52 (2018) 2178–2185.
[31] H. Li, J. Shang, Z. Yang, W. Shen, Z. Ai, L. Zhang, Oxygen vacancy associated surface Fenton chemistry: surface structure dependent hydroxyl radicals generation and substrate dependent reactivity, Environ. Sci. Technol. 51 (2017) 5685–5694.
[32] W. Ren, L. Xiong, X. Yuan, Z. Yu, H. Zhang, X. Duan, S. Wang, Activation of peroxydisulfate on carbon nanotubes: electron-transfer mechanism, Environ. Sci. Technol. 53 (2019) 14595–14603.
[33] X. Duan, H. Sun, Z. Ao, L. Zhou, G. Wang, S. Wang, Unveiling the active sites of graphene-catalyzed peroxymonosulfate activation, Carbon 107 (2016) 371–378.
[34] B. Yang, H. Kang, Y.-J. Ko, H. Woo, G. Gim, J. Choi, J. Kim, K. Cho, E.-J. Kim, S.-G. Lee, H. Lee, J. Lee, Persulfate activation by nanodiamond-derived carbon onions: effect of phase transformation of the inner diamond core on reaction kinetics and mechanisms, Appl. Catal. B Environ. 293 (2021), 120205.
[35] P. Zhang, P. Zhou, J. Peng, Y. Liu, H. Zhang, C. He, Z. Xiong, W. Liu, B. Lai, Insight into metal-free carbon catalysis in enhanced permanganate oxidation: changeover from electron donor to electron mediator, Water Res. 219 (2022), 118626.
[36] Y. Guo, Z. Zeng, Y. Li, Z. Huang, J. Yang, Catalytic oxidation of 4-chlorophenol on in-situ sulfur-doped activated carbon with sulfate radicals, Sep. Purif. Technol. 179 (2017) 257–264.